Control of astrocyte Ca^{2+} oscillations and waves by oscillating translocation and activation of protein kinase C

Franca Codazzi*, Mary N. Teruel† and Tobias Meyer†

Background: Glutamate-induced Ca^{2+} oscillations and waves coordinate astrocyte signaling responses, which in turn regulate neuronal excitability. Recent studies have suggested that the generation of these Ca^{2+} oscillations requires a negative feedback that involves the activation of conventional protein kinase C (cPKC). Here, we use total internal reflection fluorescence (TIRF) microscopy to investigate if and how periodic plasma membrane translocation of cPKC is used to generate Ca^{2+} oscillations and waves.

Results: Glutamate stimulation of astrocytes triggered highly localized GFP-PKCγ plasma membrane translocation events, induced rapid oscillations in GFP-PKCγ translocation, and generated GFP-PKCγ translocation waves that propagated across and between cells. These translocation responses were primarily mediated by the Ca^{2+}-sensitive C2 domains of PKCγ and were driven by localized Ca^{2+} spikes, by oscillations in Ca^{2+} concentration, and by propagating Ca^{2+} waves, respectively. Interestingly, GFP-conjugated C1 domains from PKCγ or PKCδ that have been shown to bind diacylglycerol (DAG) also oscillated between the cytosol and the plasma membrane after glutamate stimulation, suggesting that PKC is repetitively activated by combined oscillating increases in Ca^{2+} and DAG concentrations. The expression of C1 domains, which increases the DAG buffering capacity and thereby delays changes in DAG concentrations, led to a marked prolongation of Ca^{2+} spikes, suggesting that PKC activation is involved in terminating individual Ca^{2+} spikes and waves and in defining the time period between Ca^{2+} spikes.

Conclusions: Our study suggests that cPKCs have a negative feedback role on Ca^{2+} oscillations and waves that is mediated by their repetitive activation by oscillating DAG and Ca^{2+} concentrations. Periodic translocation and activation of cPKC can be a rapid and markedly localized signaling event that can limit the duration of individual Ca^{2+} spikes and waves and can define the Ca^{2+} spike and wave frequencies.

Addresses: *Dibit, Department of Neurosciences, S. Raffaele Scientific Institute, 20132 Milan, Italy. †Department of Molecular Pharmacology, 269 Campus Drive, Stanford University Medical Center, Stanford, California 94305, USA.

Correspondence: Tobias Meyer
E-mail: tobiasmeyer@stanford.edu

Received: **23 March 2001**
Revised: **14 May 2001**
Accepted: **23 May 2001**

Published: **24 July 2001**

Current Biology 2001, 11:1089–1097

0960-9822/01/$ – see front matter

Background

Glial cells in the central nervous system have traditionally been thought to provide structural, metabolic, and functional support for neurons. More recently, experiments in primary cultures and in brain slices showed that astrocytes, a prominent CNS subtype of glial cells, can be stimulated by neuronal activity and that they can themselves regulate the excitability of neurons. This led to the hypothesis that astrocytes are not only helper cells but are participants in neuronal communication. This hypothesis was supported by the finding that Ca^{2+} elevation in astrocytes can induce glutamate release [1] and that the released glutamate can, in turn, modulate the action potential-evoked synaptic transmission [2–4]. Different models explaining how such bidirectional neuron-astrocyte communication can be achieved (i.e., [5]) have been proposed.

An intriguing aspect of these neuronal-astrocyte communication models is the finding that astrocytes are "Ca^{2+} excitable" and that glutamate stimuli can trigger repetitive long-range Ca^{2+} waves that propagate within, as well as between, gap junction-connected astrocytes. Even though such spatially propagating Ca^{2+} waves are operating in a more than 1000-fold slower time domain than electrical signals, it is an exciting possibility that astrocyte Ca^{2+} waves serve as a means to propagate information or to coordinate the activity of spatially separated astrocytes and neurons [6, 7].

Glutamate-induced intracellular Ca^{2+} oscillations and waves in astrocytes were discovered by Smith and coworkers [8] and have since been investigated by several laboratories. At least four modes of Ca^{2+} signals can be distinguished. At low stimulus concentration and at the beginning of Ca^{2+} increases, localized Ca^{2+} spikes can typically be observed. Ca^{2+} responses can also become synchronized on a cell-wide level, resulting in two other

modes of Ca^{2+} signals: repetitive baseline Ca^{2+} spikes (Ca^{2+} spiking) separated by interspike periods in which the Ca^{2+} concentration goes back to baseline or sinusoidal-type Ca^{2+} oscillations (Ca^{2+} oscillations). The frequency of cell-wide Ca^{2+} spikes typically increases with increased receptor stimulation, and sinusoidal Ca^{2+} oscillations are often observed at higher stimulus concentration. Finally, in the fourth mode of Ca^{2+} signals, propagating Ca^{2+} waves actively spread across and between cells, a phenomena that is often observed both in single cells and in sheets of gap junction-connected cells.

Glutamate-triggered Ca^{2+} signals in astrocytes are mediated by the metabotropic glutamate receptor 5 (mGluR5), and several studies have suggested that Ca^{2+} oscillations and waves require a PKC-mediated phosphorylation of mGluR5, which reduces its coupling to G protein and phospholipase C [9–12]. Similar receptor phosphorylation mechanisms were proposed for other cell types and receptors (i.e., [13]). PKC was also shown to downregulate phospholipase C, and, in one system, a specific PKC phosphorylation site for this negative feedback has been identified in PLC-β3 [14]. This raises the important question of whether the Ca^{2+}-sensitive conventional PKC isoforms (cPKCs: α, β, and γ isoforms) are repetitively activated during Ca^{2+} oscillations and whether they can trigger the downregulation of the receptor signaling pathway after each Ca^{2+} spike. Since Ca^{2+} and DAG are coactivators of conventional PKC isoforms, it is important to understand if and how DAG levels change during Ca^{2+} oscillations and how DAG participates in generating the Ca^{2+} oscillation pattern.

Since the flat morphology of astrocytes prevented the successful use of confocal microscopy in our initial studies, we developed a total internal reflection fluorescence (TIRF) microscopy strategy [15–17] to investigate the role of conventional PKC in astrocyte Ca^{2+} oscillations and waves. This TIRF method allowed us to monitor the plasma membrane translocation of GFP-PKCγ in glutamate-stimulated hippocampal astrocytes. The biochemical similarity in the regulatory requirements of the different conventional PKC isoforms suggests that the PKCγ isoform can be used as a model for all cPKCs [18–20]. The temporal and spatial roles of DAG in PKC activation were explored by using GFP-conjugated minimal DAG binding domains (C1 and tandem C1 domains) [18, 21–24] to monitor plasma membrane DAG levels.

In this TIRF-imaging technique, a laser beam is totally internally reflected from the glass-water interface and generates an exponentially decaying excitation field (termed an evanescent wave) with a penetration depth of ~70 nm. Since the contact plasma membrane itself is only a few nm thick and is close to the glass surface, this method selectively excites GFP molecules at or near the plasma membrane, with only minimal excitation of the cytosolic GFP. Thus, the translocation of GFP constructs from the cytosol to the plasma membrane leads to an increase in fluorescence intensity since the proteins come from the dark cytosol into the evanescent wave field near the plasma membrane (see schematic panels in Figure 1). Compared to confocal microscopy, this TIRF method significantly increases the signal-to-noise for plasma membrane translocation studies and provides a new tool for translocation measurements in astrocytes and other cells with flat morphologies. Since the z-resolution is about 10-times better compared to that of confocal microscopy, the x-y-membrane distribution of fluorescent proteins can

Figure 1

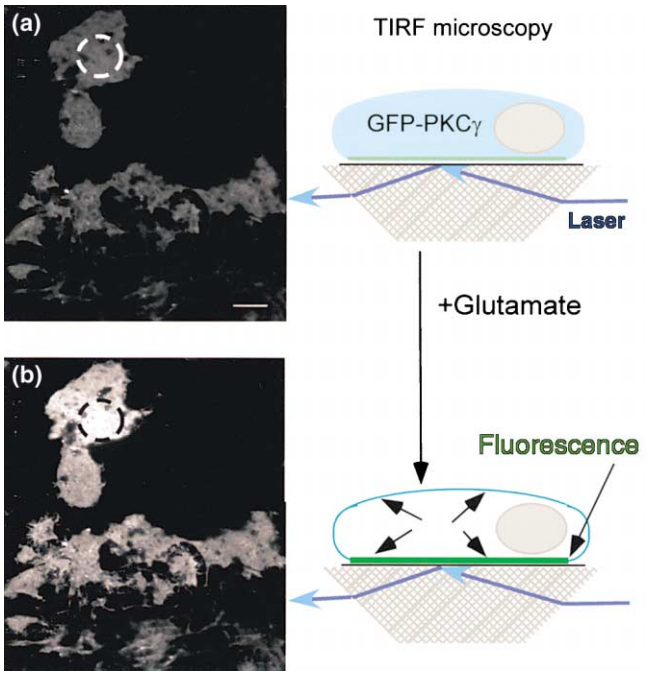

Glutamate-induced PKC translocation in hippocampal astrocytes measured by TIRF microscopy. The glutamate-induced translocation of GFP-PKCγ to the plasma membrane was measured by total internal reflection fluorescence (TIRF) microscopy. **(a)** A TIRF image of astrocytes expressing GFP-PKCγ. The fluorescence signal is weak since only a small amount of GFP-PKCγ is at or near the plasma membrane at the glass-water interface where the cells contact the coverslip. The schematic panel on the right explains the TIRF microscopy method. The laser beam is directed into the prism at such an angle that it reflects off the glass-water interface rather than passes through. This total reflection of the laser beam generates an evanescent wave field that excites GFP at or near the surface of the plasma membrane, with only minimal excitation of GFP inside the cell (within ~70 nm from the glass surface). **(b)** Glutamate-triggered translocation of GFP-PKCγ to the plasma membrane can be monitored as a marked increase in the fluorescence intensity in the TIRF image. The panel on the right shows a schematic view of how TIRF can be used to measure plasma membrane translocation. The calibration bar is 8 μm. The circular region marked in the two images was used for the time course analysis shown in Figure 2.

also be better resolved due to the absence of out-of-focus light contributions.

Using this TIRF microscopy approach combined with measurements of intracellular Ca^{2+} concentration, we found that highly localized GFP-PKCγ translocation events can occur at low stimulus intensities or at the beginning of Ca^{2+} responses, that oscillating translocations of cPKC are triggered by repetitive Ca^{2+} transients, and that cPKC translocates to the plasma membrane in waves across and between cells. Strikingly, we found that the repetitive activation of cPKC is mediated not only through Ca^{2+}-triggered translocation of the C2 domain but also by the periodic activation of the DAG binding C1 domains due to oscillations in DAG concentration. The observed oscillations in DAG concentration suggest that each Ca^{2+} spike triggers a positive Ca^{2+} feedback onto phospholipase C, which in turn generates additional DAG. The synergistic production of DAG and Ca^{2+} signals, and the resulting activation of PKC, leads to a delayed termination of individual Ca^{2+} spikes and to a prolonged downregulation that can define the time period until the next Ca^{2+} spike is triggered. Furthermore, the expression of DAG buffers as well as increased concentrations of cPKC alter the pattern of Ca^{2+} spikes and waves, suggesting that PKC is activated repetitively by oscillations of both of its coactivators, Ca^{2+} and DAG, and indeed has a critical negative feedback role in generating Ca^{2+} oscillations.

Results and discussion

Role of cPKCs in generating astrocyte Ca^{2+}-spiking patterns

We investigated how conventional PKC isoforms may participate in the regulation of glutamate-induced Ca^{2+} oscillations by monitoring the plasma membrane translocation of an expressed GFP-conjugated PKCγ isoform (GFP-PKCγ) [23, 25]. In these experiments, cultured hippocampal astrocytes (1–2 weeks in culture) were transfected with the PKC constructs by microporation [26]. The glutamate-induced GFP-PKCγ translocation to and its dissociation from the plasma membrane were analyzed by selective illumination of the surface plasma membrane using total internal reflection fluorescence microscopy (Figure 1). In this microcopy method, the cellular fluorescence is very low for cytosolic GFP-PKCγ (Figure 1a) and becomes several-fold stronger after the PKC isoform translocates to the plasma membrane following glutamate stimulation (Figure 1b). A schematic view of the TIRF principle for translocation imaging is shown in panels on the right of the images.

In all cells expressing GFP-PKCγ, the addition of 100 μM glutamate resulted in a significant increase in fluorescence intensity at the plasma membrane, and strikingly, in most of the series of TIRF images analyzed (n = 21 out of 29 experiments), the increases were repetitive. This suggests that GFP-PKCγ translocates repetitively to the plasma membrane in response to glutamate stimuli (Figure 2a, upper trace). The traces in Figure 2 were obtained by monitoring the average fluorescence intensity at a cell surface region as a function of time (the region used for this trace is shown in Figure 1). The two images shown in Figure 1a and 1b were taken at the time points marked in the upper trace in Figure 2a. The oscillatory pattern of fluorescence intensity changes was also observed at lower glutamate concentration (10 μM) and in extracellular buffer without Ca^{2+} (data not shown). In control measurements, glutamate addition to cells expressing the GFP protein alone or a plasma membrane-targeted GFP with a fused palmitoylation/myristoylation sequence (PM-GFP) [26] did not induce significant changes in fluorescence intensity. This excludes the possibility that the observed fluorescence intensity changes of GFP-PKCγ are caused by cell movement and not by the plasma membrane translocation of the kinase itself (data not shown). The behavior of GFP-PKCγ was representative for all cPKCs, since astrocytes transfected with GFP-PKCα and GFP-PKCβI showed the same type of oscillating translocation after glutamate stimulation (data not shown).

In order to understand how Ca^{2+} signals and PKC translocation relate to each other, we measured GFP-PKCγ translocation in parallel with the concentration of intracellular Ca^{2+} [18, 20]. These dual measurements were achieved by microporating the GFP-PKCγ construct together with the red-shifted Ca^{2+} dye Ca^{2+} Crimson. In these measurements, the light path and wavelength were rapidly switched between the TIRF-excited GFP-PKCγ signal and the epifluorescence-excited Ca^{2+} dye (see Materials and methods). Using this method, glutamate-stimulated astrocytes showed a marked temporal correlation between the intracellular Ca^{2+} spikes and GFP-PKCγ translocation (Figure 2a), suggesting that each upstroke in intracellular Ca^{2+} triggers a translocation of GFP-PKCγ to the plasma membrane.

When Ca^{2+} responses were analyzed for the same glutamate concentration in astrocytes that did not express GFP-PKCγ, a smaller number of cells had oscillating or repetitive spiking responses (43% of the experiments, n = 6 out of 14 experiments, compared to 72%, or n = 21 out of 29 experiments). Also, the oscillatory Ca^{2+} responses in cells without GFP-PKCγ had a dampened sinusoidal pattern (Figure 2b; two typical traces are shown) rather than a pattern of repetitive baseline spikes, as seen in cells that had GFP-PKCγ expressed (for example, Figure 2a). This suggests that an increase in cellular cPKC concentration might strengthen a negative feedback component that brings Ca^{2+} levels back to baseline after each Ca^{2+} spike.

Figure 2

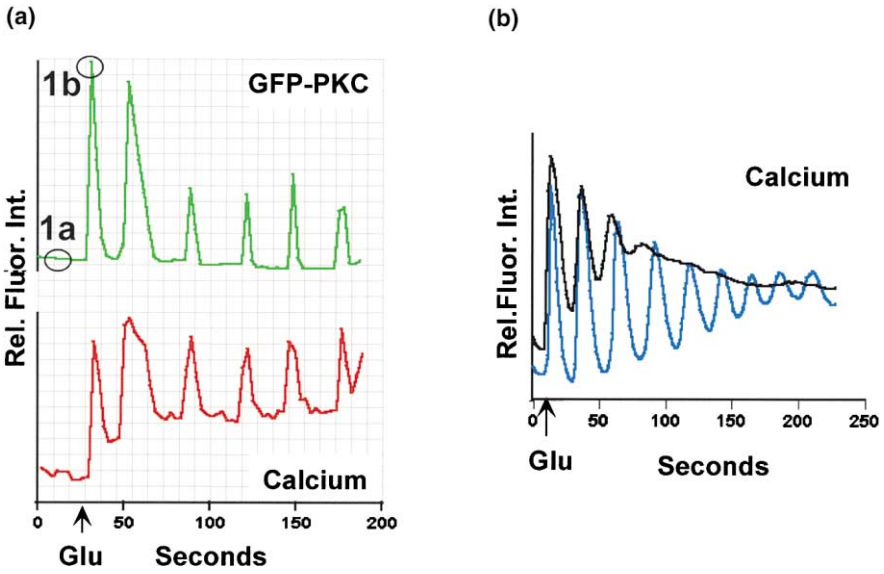

A time course of glutamate-induced GFP-PKCγ translocation versus a time course of Ca^{2+} signals in hippocampal astrocytes. **(a)** The time course analysis of repetitive GFP-PKCγ translocations (green trace) compared to the time course of intracellular Ca^{2+} oscillations measured with Ca^{2+} Crimson (red trace) resulting from the addition of 100 μM glutamate (final concentration). These dual measurements were made by rapidly switching between TIRF-excited GFP images (excitation: 488 nm) and epifluorescence-excited Ca^{2+} Crimson images (excitation: 568 nm). The images shown in Figure 1 represent the GFP-PKCγ fluorescence in the basal condition (Figure 1a) and during maximal translocation (Figure 1b). The time points when the images were taken are marked in the GFP-PKCγ trace. The relative fluorescence intensity represented by both traces was measured in the circular region marked in Figure 1. The maximum change in the relative fluorescence intensity was 1.2 for the GFP-PKCγ trace and 0.2 for the calcium trace. **(b)** The time course of intracellular Ca^{2+} concentration changes induced by glutamate (100 μM) in two astrocytes loaded with the Ca^{2+} fluorescent dye Fluo-3AM and analyzed by confocal microscopy. The oscillatory pattern shown was seen in 6 out of 14 experiments, with single transients and plateaus observed in the other experiments. The maximum change in relative fluorescence intensity was 1.5.

Propagation of GFP-PKCγ translocation waves and local GFP-PKCγ translocation sites

When several transfected astrocytes were present in the field of view, the analysis of a series of TIRF images showed that glutamate stimulation induced repetitive GFP-PKCγ fluorescent waves that propagated across and between cells (Figure 3a, see Movie 1 in the Supplementary material available with this article online). This implies that cPKC's translocation to the plasma membrane occurs in the form of translocation waves. These translocation waves are likely driven by the glutamate-induced intra- and intercellular Ca^{2+} waves observed previously [8, 27, 28]. The propagation rate for PKC translocation of 10–20 μm/s at room temperature is similar to the previously measured propagation rates for Ca^{2+} waves.

In most experiments, the repetitive translocation waves originated at a defined plasma membrane site where the translocation of GFP-PKCγ was often more persistent, was asynchronous, or preceded the repetitive translocations in the rest of the cell (Figure 3b, see Movie 1 in the Supplementary material). In order to investigate such local translocation hot spots at the plasma membrane, we utilized a construct that fused GFP with the PKCγ C2 domain, a minimal Ca^{2+} and lipid binding domain that has been shown to translocate to the plasma membrane in response to Ca^{2+} signals and not to DAG signals (GFP-C2γ) [18, 29]. In astrocytes expressing GFP-C2γ, TIRF microscopy revealed transient micrometer-sized fluorescent spots that could best be observed in basal conditions (Figure 3c) or in the presence of weak stimuli. When stimulated at high glutamate concentrations, astrocytes expressing GFP-C2 showed cell-wide repetitive translocations and translocation waves with patterns similar to those of GFP-PKCγ. This suggests that the local hot spots of PKC plasma membrane translocation events result from local Ca^{2+} spikes [30, 31] and that a main driving force for local, as well as cell-wide, cPKC translocation is the increase in Ca^{2+} concentration. The observed discrete sites of C2 domain translocation suggest that local "target activation units" exist at the astrocyte plasma membrane and that such sites can also serve as origination points for Ca^{2+} waves [32].

Glutamate-induced oscillations in the translocation of GFP-conjugated C1 domains that bind DAG

Biochemical studies have shown that Ca^{2+}-induced binding of conventional PKC isoforms to lipid membranes induces only minimal PKC activation and that full activation requires the binding of the coactivator DAG [22]. During baseline Ca^{2+} spiking or Ca^{2+} oscillations, two possible scenarios may apply. First, the level of DAG may be constant or may increase slowly after glutamate stimulation, and cPKCs would then be activated by repetitive Ca^{2+}-C2 domain-mediated translocation. In the second hypothesis, a previously shown Ca^{2+}-dependence of phospholipase C activity may lead to parallel oscillations in the DAG concentration, which would result in repetitive C1 and C2 domain-mediated cPKC activation and inactivation that depends on the repetitive increase and

Figure 3

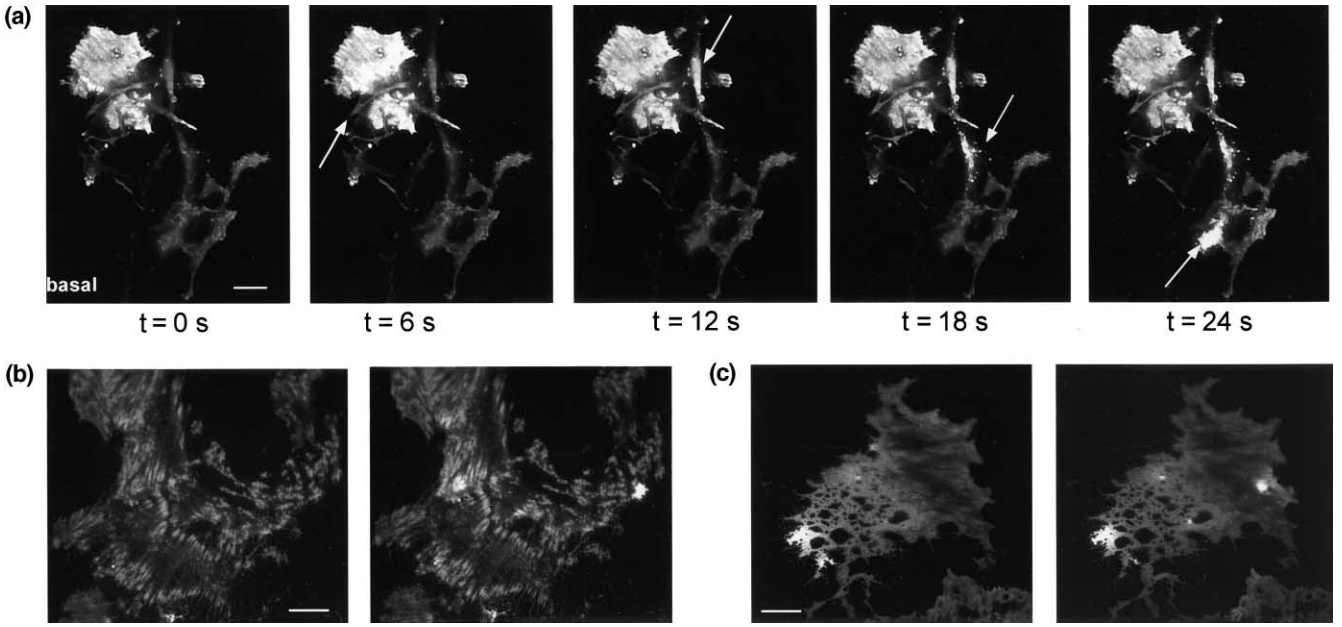

Local GFP-PKCγ and GFP-C2 domain translocation events and propagating translocation waves. **(a)** The glutamate (100 μM)-triggered plasma membrane translocation of GFP-PKCγ propagated across the cell surface as intra- and intercellular waves. A series of images was taken from a longer recording and is shown as consecutive panels. The images shown were taken 6 s apart, and the arrows mark the propagation of a GFP-PKCγ translocation wave. **(b)** Local GFP-PKCγ translocation events were often observed both at basal conditions or after glutamate stimulation. An example of such local translocations can be seen in the right panel taken 2 min after glutamate stimulation (100 μM). **(c)** An example of spontaneous local GFP-C2 domain translocation events occurring with the astrocytes at basal condition. The calibration bars represent 5 μm.

decrease of Ca^{2+}, as well as DAG. The second mechanism would provide a much sharper on-and-off process for repetitive PKC activation during Ca^{2+} oscillations. We tested these two hypotheses by using GFP-conjugated DAG binding domains as fluorescent biosensors for plasma membrane-generated DAG.

The structure of one of the C1 domains of PKC-δ has been solved [21], and biochemical studies have shown that the tandem domain has high affinity for diacylglycerol. When compared to the C1 domain from PKCγ, GFP-conjugated tandem C1 domains from PKCδ showed a stronger translocation signal in response to the addition of submaximal concentration of DiC8 (a DAG analog) (data not shown). We therefore used the GFP-conjugated PKCδ $C1_2$ domain to monitor glutamate-triggered DAG production in astrocytes. In cells that express GFP-$C1_2$δ, the addition of glutamate (100 μM or 1 mM) induced a rapid increase in TIRF fluorescence, suggesting that functionally relevant amounts of DAG are generated by glutamate. Strikingly, the fluorescent signal propagated across the cell (see Movie 2 in the Supplementary material) in similar fashion to the signals observed in cells expressing GFP-PKCγ. Translocation events also appeared to be highly localized in many cases. Oscillating translocations of the DAG biosensor occurred in 15 out of 21 experiments. Furthermore, in 9 of the 15 experiments in which translocation was observed, maximal glutamate administration (100 μM–1 mM) triggered an initial rapid translocation of the DAG biosensor, followed by a series of repetitive translocations (Figure 4b). This finding that glutamate triggers repetitive translocation and spatial propagation of the DAG binding domain suggests that changes in Ca^{2+} and DAG concentrations are indeed functionally coupled and may lead to oscillating coincidence signals and a resulting steep and repetitive cPKC activation.

We also found that the GFP-$C1_2$δ domain probe translocated to the plasma membrane after the addition of the Ca^{2+} ionophore ionomycin (0.5–1 μM). This increase in fluorescence was not an artifact, since ionomycin addition to astrocytes expressing cytosolic GFP or myristoylated/palmitoylated PM-GFP did not show this increase (data not shown). The ionomycin-triggered C1 domain translocation could be explained by a production of DAG via the activation of Ca^{2+}-sensitive PLC, or by an unknown Ca^{2+} binding site on GFP-$C1_2$δ. However, the available crystal structure of one of the C1 domains of GFP-$C1_2$δ does not indicate that such a Ca^{2+} binding site exists [21]. Since control measurements with an inhibitor of PLC (U73122) were inconclusive (U73122 caused Ca^{2+} in-

Figure 4

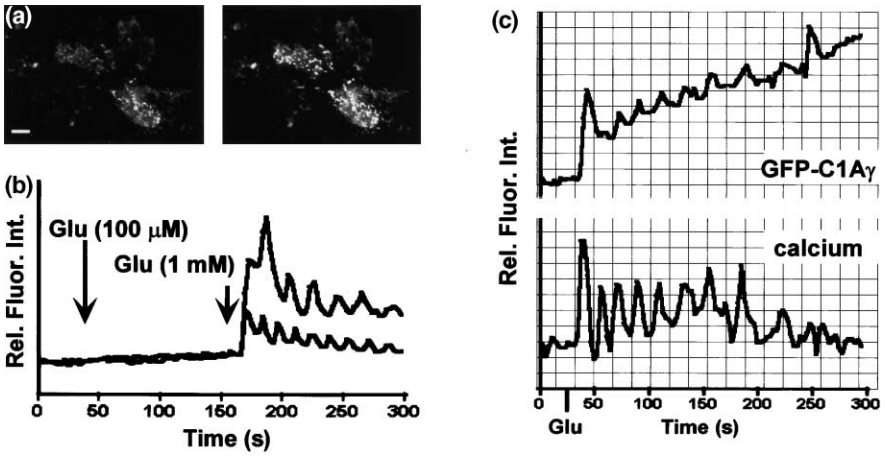

Glutamate-induced oscillating translocation of DAG binding C1 domains. **(a)** Glutamate stimulation (1 mM) induced a marked plasma membrane translocation of the tandem DAG binding C1 domains of PKCδ (GFP-$C1_2$δ). The left and right panels show images taken before and after maximal translocation occurred. **(b)** The oscillating time course of the GFP-$C1_2$δ fluorescence intensity change in the two astrocytes shown in (a). The calibration bar represents 5 μm. Similar oscillations were observed in 9 out of 21 experiments. The maximum change in relative fluorescence intensity was 0.3. **(c)** The time course of plasma membrane translocation of a single DAG binding C1 domain from PKCγ (GFP-C1Aγ) measured in parallel with cytosolic Ca^{2+} oscillations after glutamate stimulation (1 mM). The GFP and the Ca^{2+} Crimson fluorescent recordings were performed as described in Figure 2a. In 4 out of 8 experiments, the GFP-C1Aγ showed a similar oscillating pattern, with each translocation event being preceded by a Ca^{2+} spike. The maximum change in relative fluorescence intensity was 0.2 for the GFP-C1Aγ trace and 0.2 for the calcium trace.

creases itself), we used a GFP-conjugated single C1 domain (C1A, also termed Cys-domain) from PKCγ as an alternative DAG binding construct (GFP-C1Aγ) [23]. Even though this probe has a lower affinity for DAG, half of the responsive astrocytes exhibited repetitive translocations of this C1A DAG biosensor (n = 4, out of 8 experiments). The remaining cells responded with a single fluorescence increase. In the experiment shown in Figure 4c, in which dual DAG and Ca^{2+} measurements were performed, the Ca^{2+} increases precede the GFP-C1Aγ translocation to the plasma membrane. Together with the data from the tandem C1 domain from PKCδ, these measurements suggest that oscillations in DAG concentrations occur and that oscillating Ca^{2+}, as well as DAG, concentrations trigger the repetitive activation of cPKCs. Thus, the observed oscillations in DAG and Ca^{2+} signals and the marked effect of increasing PKC concentration on Ca^{2+} oscillations described above support the hypothesis that repetitive PKC activation is a key control element of the astrocyte Ca^{2+}-signaling response.

Expression of GFP-$C1_2$δ alters the duration of Ca^{2+} spikes and the pattern of Ca^{2+} oscillations

If changes in DAG concentration are indeed important for generating the repetitive Ca^{2+}-signal patterns, the expression of increased concentrations of C1 domains should alter the shape and frequency of Ca^{2+} spikes since the C1 domains act as a buffer for DAG, which should in turn slow changes in DAG concentration. As discussed above, oscillating translocations of the PKCδ-C1 tandem biosensor (GFP-$C1_2$δ) were observed in 15 out of 21 experiments after glutamate stimulation. In 9 of the 15 experiments in which translocation occurred, rapid-oscillating GFP-$C1_2$δ translocation was observed (Figure 4b). However, in the remaining 6 out of 15 experiments, the TIRF microscopy analysis revealed a limited number of much slower GFP-$C1_2$δ translocation events and Ca^{2+} transients. For these transient Ca^{2+} increases, the upstroke of the GFP-$C1_2$δ translocations was fast, whereas the recovery time for Ca^{2+} signals and translocation was much slower, requiring more than 25 s to drop back near the basal level. Moreover, in these cells, a higher amplitude of the relative fluorescence increase suggested that more DAG was produced during each transient in these cells (Figure 5, upper panel), suggesting that the buffering of DAG by the GFP-$C1_2$δ probe delays the physiological inactivation of PLC by slowing the activation of PKC. The longer duration and the higher amplitude can best be explained by such a buffering effect on DAG.

When the timing between Ca^{2+} signals and C1 domain translocation was directly compared, the measured Ca^{2+} and DAG signals showed a similar overall time course. However, in a comparison of 16 Ca^{2+} spikes in which both fluorescent signals were well resolved, Ca^{2+} increased first, and the GFP-$C1_2$δ translocation started seconds later once the intracellular Ca^{2+} level reached an apparent threshold value (Figure 5, lower panel). This suggests that the Ca^{2+}-mediated activation of PLC and the resulting production of DAG are triggered once a critical Ca^{2+} level is reached.

Figure 5

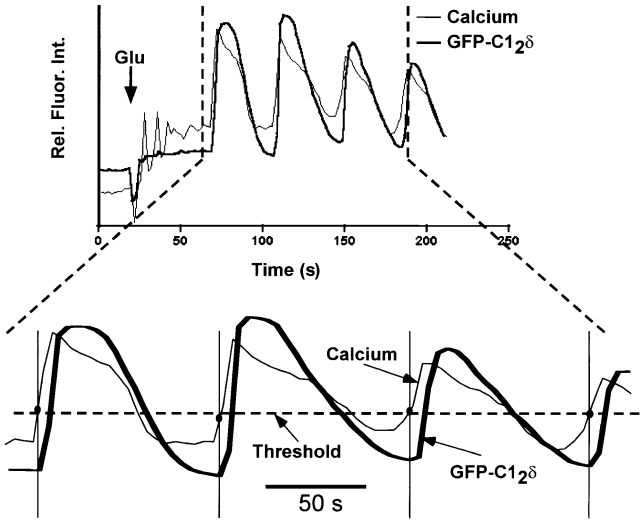

The effect of the expression of the tandem DAG binding domains of PKCδ ($C1_2\delta$) on shape and duration of Ca^{2+} oscillations. Parallel measurements of GFP-$C1_2\delta$ translocation and Ca^{2+} signals in an astrocyte that exhibited slow baseline Ca^{2+} spikes. This type of slow Ca^{2+} transient was not observed in astrocytes in the absence of C1 domain expression. The two superimposed traces in the upper panel show a comparison of the time courses of Ca^{2+} spikes and repetitive plasma membrane translocation of GFP-$C1_2\delta$ after stimulation with 100 μM glutamate. The magnified view in the lower panel shows that the translocation of the C1 domain is delayed by a few seconds and that the GFP-$C1_2\delta$ translocation is triggered only after reaching a threshold in Ca^{2+} concentration. The maximum change in relative fluorescence intensity was 1.3 for the GFP-$C1_2\delta$ trace and 0.45 for the calcium trace.

Figure 6

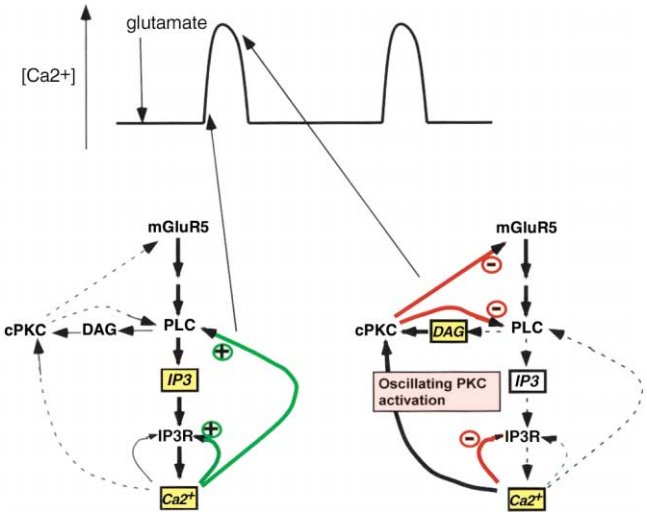

Periodic PKC activation as a negative feedback mechanism that supports the generation of astrocyte Ca^{2+} oscillations and waves. A proposed model of the positive and negative feedback mechanisms that control baseline Ca^{2+} spiking, Ca^{2+} oscillations, and waves. The two positive feedbacks that participate in the upstroke of each Ca^{2+} transient are shown on the left. DAG and IP3 are both expected to oscillate in this model, with each increase in IP3 and DAG being driven by Ca^{2+} activation of PLC. As shown in the schematic view on the right, periodic desensitization of the GPCR pathway by cPKC is then expected to support the termination of each Ca^{2+} spike by phosphorylating the GPCR, PLC, and other upstream signaling proteins. The same cPKC-mediated phosphorylation events would then generate a prolonged downregulation with a recovery rate that defines the time period (frequency) when the subsequent Ca^{2+} spike is triggered.

Model for a role of oscillating Ca^{2+} and DAG concentrations for generating repetitive Ca^{2+} transients and waves

How can these results be put together with our current knowledge of Ca^{2+} regulatory mechanisms? Figure 6 shows a model of the feedback loops that are likely significant in astrocytes and may explain how glutamate stimuli can drive Ca^{2+} oscillations, Ca^{2+} spiking, and Ca^{2+} waves. The previously described positive feedbacks from Ca^{2+} onto IP3-receptors and onto PLC are shown in green in the left panel [33–36]. A direct and rapid negative feedback of Ca^{2+} onto the IP3-receptor is shown in red (i.e., [37–39]). Our study now suggests that cPKCs are involved in mediating at least two additional negative feedbacks that are critical for controlling astrocyte Ca^{2+} signals (shown in red in the right panel).

We propose that cPKCs, which require Ca^{2+} for translocation and DAG for activation, are activated in a periodic fashion during Ca^{2+} oscillations, spiking, or waves. In this model, a delayed on-and-off-type mechanism for cPKC activation is mediated by repetitive engagement of its C1 and C2 domains due to oscillations of the two coactivators, Ca^{2+} and DAG. Our earlier mechanistic study of PKC activation [18] suggested that the DAG binding to the plasma membrane-localized PKC is delayed by several seconds even if DAG is present in the plasma membrane. More interestingly, the now measured delayed increase in the translocation of C1 domains, reported here, suggests that Ca^{2+} rapidly activates PLC to generate more DAG during each Ca^{2+} transient, providing a safeguard to limit PKC activity before a Ca^{2+} transient is well under way.

The previously observed delayed binding of DAG to PKC [18], combined with the now observed delayed increase in DAG concentration, allows for a potent delay in PKC activation so that PKC only becomes active a few seconds after the Ca^{2+} transient is triggered. The activated PKC can then phosphorylate targets such as the inhibitory threonine 840 in the C-terminal region of mGluR5 [9] or the serine 1105 site on PLC-β3 [14], and thereby participate in terminating individual Ca^{2+} spikes and waves. A second likely role for cPKC-mediated phosphorylation is to delay the triggering of the subsequent Ca^{2+} spike by a prolonged downregulation of the signaling system. The resulting delayed time period for triggering the next Ca^{2+}

spike would then be primarily defined by the reversal of the cPKC-mediated phosphorylation.

Overall, our study suggests that the upstroke of astrocyte Ca^{2+} spikes are triggered by two positive feedbacks, a Ca^{2+} activation of IP3-receptors and a Ca^{2+} activation of PLC, which in turn produces more IP3. In turn, the delayed activation of cPKC by Ca^{2+} and DAG during each Ca^{2+} increase leads to the downregulation of PLC and supports the termination of each Ca^{2+} transient. The recovery from this PKC-mediated downregulation then defines the frequency at which repetitive spikes are triggered.

Conclusions

Our TIRF microscopy studies show that the plasma membrane translocation of conventional PKC can be controlled by an intricate spatial and temporal regulatory process. TIRF microscopy, the imaging method used for this analysis, was found to be a powerful new tool to investigate such translocation events. The observed oscillations in PKCγ translocation, the spatial propagation of PKCγ translocation waves, as well as the hot spots of local PKCγ translocation appear to be predominantly driven by corresponding Ca^{2+} signals. A surprising observation was that rapid and highly localized translocation events can occur, thus suggesting that local units of PKC activation can be induced by local second messenger signals. Finally, the observed oscillating translocations of the DAG binding C1 domains suggest that PKC can be activated in a repetitive manner by oscillating Ca^{2+}, as well as DAG, signals and that the repetitive activation of PKC is a key mechanism for defining the shape of Ca^{2+} spikes and the frequency at which they are triggered.

Materials and methods

Cell culturing

Primary hippocampal astrocytes were imaged in mixed neuron/glia cocultures, obtained from 3- to 4-day-old Sprague-Dawley rats, as described [26]. Briefly, after the quick subdivision of the hippocampi into small sections, the tissue was incubated into a digestion solution consisting of 10 μg/ml trypsin type IX (Sigma) and 0.5 μg/ml DNase type IV (Sigma). The pieces were then mechanically dissociated in a Hank's solution supplemented with 12 mM $MgSO_4$ and 0.5 μg/ml Dnase type IV. After centrifugation, the cells were plated onto Matrigel-coated coverslips and maintained in MEM (GIBCO) supplemented with 0.6% glucose, 1 mM $NaHCO_3$, 2.4 g/l transferrin (Calbiochem), 0.25 g/l insulin (Sigma), 0.3 g/l glutamine, 5% fetal calf serum (Hyclone), and 8 mM AraC. The cultures were maintained at 37°C in a 95% air-, 5% CO_2-humidified incubator and were used 7–14 days after plating.

Cloning of GFP fusion constructs and electroporation

The $C1_2$ domains of PKCδ were amplified by PCR, and the PCR products were cloned into EGFP vectors from Clontech. The PM-GFP construct that uses the C-terminal palmitoylation/myristoylation sequence from Lyn to target GFP to the plasma membrane was described in [26]. The cloning of the full-length rat PKCγ and PKCγ-C1A domain GFP fusion constructs was described in [23].

The cDNA constructs, in some cases together with the fluorescent Ca^{2+} dye dextran (70 kDa) Ca^{2+} Crimson, were electroporated into adherent cells using a 1 μl microporation device for adherent cells [26]. Electroporation was performed at 340 V/cm using three rectangular voltage pulses, each of which was 100 ms long and 20 s apart. After electroporation, the cells were placed in serum-containing medium and left for at least 12 hr at 37°C and 5% CO_2.

Total internal reflection fluorescence (TIRF) microscopy (also termed evanescent wave microscopy)

The use of evanescent wave excitation for biological studies was introduced by Axelrod in 1981 [15]. We set up a TIRF microscope for our measurements with the following criterion: capability of long-term live cell imaging, access to cells during experiments, the ability of using different magnifications, as well as the capability to switch between TIRF and epifluorescence with different excitation wavelengths. The setup has been built around a Zeiss Axioskope 2 microscope, with the laser excitation beam entering from below the coverslip through a fixed dove prism (Edmund Scientific) [40]. The laser beam went through the prism and the glass of the coverslip, which was optically coupled to the prism by microscope immersion oil with the same refractive index (1.52) so that the total internal reflection occurred at the glass-water interface. The angle used for total internal reflection (∼20°) was calculated to produce an exponentially decaying intensity field in the cell above the glass surface with a space constant of ∼70 nm. Cells were grown on 25 mm circular coverslips in a chamber enclosed by a 3-mm-wide and 3-mm-high teflon ring that contained the extracellular buffer solution. The chamber was directly mounted on a motor controlled x-y-stage, and its movement did not disrupt the ∼200 μm thick oil connection between the coverslip and the prism. The cells were magnified by a water-immersion objective (40× or 63×, Zeiss)

The cells expressing GFP fusion constructs were excited using a 488 nm laser line (Coherent, Auburn Group, typically 50–100 mW) and a 500-nm-long pass filter for emission. The light emitted by the fluorescent proteins was collected by a cooled CCD videocamera (Princeton Instruments Micromax, 5 MHz). Time series of images were recorded before, during, and after cell stimulation using Metamorph software (Universal Imaging). In all plots, "Relative fluorescence intensity" was calculated for the cell, or other regions of interest, as (maximum fluorescence intensity − minimum fluorescence intensity)/minimum fluorescence intensity. All intensity values were obtained after background subtraction.

All experiments were made at room temperature. Before each experiment, the coverslips were washed three times with an extracellular buffer (5 mM KCl, 125 mM NaCl, 20 mM HEPES [pH 7.4], 1.5 mM $CaCl_2$, 1.5 mM $MgCl_2$, and 10 mM glucose). All added substances were dissolved or diluted in the same buffer.

When the GFP construct translocations were measured concurrently with intracellular Ca^{2+} concentration, a second argon/krypton ion laser was used to excite the Ca^{2+} dye Ca^{2+} Crimson (excitation 568 nm) through the epifluorescence pathway. The two emitted wavelengths were transmitted by a custom-made dichroic mirror and by two emission filters (500-nm-long pass for GFP, and 590-nm-long pass for Ca^{2+} Crimson) placed in a software-controlled BioPoint filter wheel. The shutters (to alternate the excitation pathways) and the position of the filter wheel were controlled by Metamorph software (Universal Imaging). Since the evanescent wave and the epifluorescence excitation were used sequentially, the two fluorescent spectra had only an insignificant overlap.

Supplementary material

Supplementary material including Movies 1 and 2, showing the repetitive propagating signal of GFP-PKCγ and GFP-$C1_2$δ, respectively, is available at http://images.cellpress.com/supmat/supmatin.htm.

Acknowledgements

We thank the members of the Grohovaz and Meyer lab for helpful discussions. This work was supported by a Human Frontier Science Program fellowship SF0023/1998-M to F.C., a National Institutes of Health fellowship 1F32NS10767-01 to M.N.T., and National Institutes of Health grants GM48113, GM51457, and CA83229 to T.M.

References

1. Bezzi P, Carmignoto G, Pasti L, Vesce S, Rossi D, Lodi Rizzini B, *et al.*: **Prostaglandins stimulate calcium-dependent glutamate release in astrocytes.** *Nature* 1998, **391:**281-285.
2. Araque A, Parpura V, Sanzgiri RP, Haydon PG: **Glutamate-dependent astrocyte modulation of synaptic transmission between cultured hippocampal neurons.** *Eur J Neurosci* 1998, **10:**2129-2142.
3. Parpura V, Basarsky TA, Liu F, Jeftinija K, Jeftinija S, Haydon PG: **Glutamate-mediated astrocyte-neuron signalling.** *Nature* 1994, **369:**744-747.
4. Nedergaard M: **Direct signaling from astrocytes to neurons in cultures of mammalian brain cells.** *Science* 1994, **263:**1768-1771.
5. Pasti L, Volterra A, Pozzan T, Carmignoto G: **Intracellular calcium oscillations in astrocytes: a highly plastic bidirectional form of communication between neurons and astrocytes in situ.** *J Neurosci* 1997, **17:**7817-7830.
6. Dani JW, Chernjavsky A, Smith SJ: **Neuronal activity triggers Ca2+ waves in hippocampal astrocyte networks.** *Neuron* 1992, **8:**429-440.
7. Porter JT, McCarthy, KD: **Hippocampal astrocytes in situ respond to glutamate released from synaptic terminals.** *J Neurosci* 1996, **16:**5073-5081.
8. Cornell-Bell AH, Finkbeiner SM, Cooper MS, Smith SJ: **Glutamate induces calcium waves in cultured astrocytes: long-range glial signaling.** *Science* 1990, **247:**470-473.
9. Kawabata S, Tsutsumi R, Kohara A, Yamaguchi T, Nakanishi S, Okada M: **Control of calcium oscillations by phosphorylation of metabotropic glutamate receptors.** *Nature* 1996, **383:**89-92.
10. Kawabata S, Kohara A, Tsutsumi R, Itahana H, Hayashibe S, Yamaguchi T, Okada M: **Diversity of calcium signaling by metabotropic glutamate receptors.** *J Biol Chem* 1998, **273:**17381-17385.
11. Nakahara K, Okada M, Nakanishi S: **The metabotropic glutamate receptor mGluR5 induces calcium oscillations in cultured astrocytes via protein kinase C phosphorylation.** *J Neurochem* 1997, **69:**1467-1475.
12. Macek TA, Schaffhauser H, Conn PJ: **Protein kinase C and A3 adenosine receptor activation inhibit presynaptic metabotropic glutamate receptor (mGluR) function and uncouple mGluRs from GTP-binding proteins.** *J Neurosci* 1998, **18:**6138-6146.
13. Bird GJ, Rossier MF, Obie JF, Putney JW: **Sinusoidal oscillations in intracellular calcium requiring negative feedback by protein kinase C.** *J Biol Chem* 1993, **268:**8425-8428.
14. Yue C, Ku CY, Liu M, Simon MI, Sanborn BM: **Molecular mechanism of the inhibition of phospholipase C 3 by protein kinase C.** *J Biol Chem* 2000, **275:**30220-30225.
15. Axelrod D: **Cell-substrate contacts illuminated by total internal reflection fluorescence.** *J Cell Biol* 1981, **89:**141-145.
16. Oheim M, Loerke D, Stuhmer W, Chow RH: **The last few milliseconds in the life of secretory granules. Docking, dynamics and fusion visualized by total internal reflection fluorescence microscopy (TIRFM).** *Eur Biophys J* 1998, **27:**83-98.
17. Funatsu T, Harada Y, Tokunaga M, Saito K, Yanagida T: **Imaging of single fluorescent molecules and individual ATP turnover by single myosin molecules in aqueous solution.** *Nature* 1995, **374:**555-559.
18. Oancea E, Meyer T: **Protein kinase C as a molecular machine for decoding calcium and DAG signals.** *Cell* 1998, **95:**307-318.
19. Feng X, Zhang J, Barak LS, Meyer T, Caron MG, Hannun YA: **Visualization of dynamic trafficking of a protein kinase C betaII/green fluorescent protein conjugate reveals differences in G protein-coupled receptor activation and desensitization.** *J Biol Chem* 1998, **273:**10755-10762.
20. Almholt K, Arkhammar PO, Thastrup O, Tullin S: **Simultaneous visualization of the translocation of protein kinase Calfa-green fluorescent protein hybrids and intracellular calcium concentration.** *Biochem J* 1999, **337:**211-218.
21. Zhang G, Kazanietz MG, Blumberg PM, Hurley JH: **Crystal structure of the cys2 activator-binding domain of protein kinase C delta in complex with phorbol ester.** *Cell* 1995, **81:**917-924.
22. Nishizuka Y: **Protein kinase C and lipid signaling for sustained cellular responses.** *FASEB J* 1995, **9:**484-496.
23. Oancea E, Teruel MN, Quest AF, Meyer T: **Green fluorescent protein (GFP)-tagged cysteine-rich domains from protein kinase C as fluorescent indicators for DAG signaling in living cells.** *J Cell Biol* 1998, **140:**485-498.
24. Ron D, Kazanietz MG: **New insights into the regulation of protein kinase C and novel phorbol ester receptor.** *FASEB J* 1999, **13:**1658-1674.
25. Sakai N, Sakai K, Ikegaki N, Shirai Y, Ono Y, Saito N: **Direct visualization of the translocation of the gamma-subspecies of protein kinase C in living cells using fusion proteins with green fluorescent protein.** *J Cell Biol* 1997, **139:**1465-1476.
26. Teruel MN, Blanpied TA, Shen K, Augustine GJ, Meyer T: **A versatile microporation technique for the transfection of cultured CNS neurons.** *J Neurosci Methods* 1999, **93:**37-48.
27. Charles AC, Merrill JE, Dirksen ER, Sanderson MJ: **Intercellular signaling in glial cells: calcium waves and oscillations in response to mechanical stimulation and glutamate.** *Neuron* 1991, **6:**983-992.
28. Cotrina ML, Lin JH, Alves-Rodrigues A, Liu S, Li J, Azmi-Ghadimi H, *et al.*: **Connexins regulate calcium signaling by controlling ATP release.** *Proc Natl Acad Sci USA* 1998, **95:**15735-15740.
29. Verdaguer N, Corbalan-Garcia S, Ochoa WF, Fita I, Gomez-Fernandez JC: **Ca2+ bridges the C2 membrane binding domain of protein kinase Calfa directly to phosphatidylserine.** *EMBO J* 1999, **18:**6329-6338.
30. Horne JH, Meyer T: **Elementary calcium-release units induced by inositol trisphosphate.** *Science* 1997, **276:**1690-1693.
31. Bootman MD, Berridge MJ, Lipp P: **Cooking with calcium: the recipes for composing global signals from elementary events.** *Cell* 1997, **91:**367-373.
32. Yagodin SV, Holtzclaw L, Sheppard CA, Russel JT: **Nonlinear propagation of agonist-induced cytoplasmic calcium waves in single astrocytes.** *J Neurobiol* 1994, **25:**265-280.
33. Meyer T, Stryer L: **Molecular model for receptor-stimulated calcium spiking.** *Proc Natl Acad Sci USA.* 1988, **85:**5051-5055.
34. Goldbeter A, Dupont G, Berridge MJ: **Minimal model for signal-induced Ca2+ oscillations and for their frequency encoding through protein phosphorylation.** *Proc Natl Acad Sci USA.* 1990, **87:**1461-1465.
35. Berridge M, Lipp P, Bootman M: **Calcium signaling.** *Curr Biol* 1999, **9:**R157-R159.
36. Hirose K, Kadowaki S, Tanabe M, Takeshima H, Iino M: **Spatiotemporal dynamics of inositol 1,4,5-trisphosphate that underlies complex Ca2+ mobilization patterns.** *Science* 1999, **284:**1527-1530.
37. Adkins CE, Taylor CW: **Lateral inhibition of inositol 1,4,5-trisphosphate receptors by cytosolic Ca(2+).** *Curr Biol* 1999, **9:**1115-1118.
38. Miyakawa T, Mizushima A, Hirose K, Yamazawa T, Bezprozvanny I, Kurosaki T, *et al.*: **Ca2+-sensor region of IP3 receptor controls intracellular Ca2+ signaling.** *EMBO J* 2001, **20:**1674-1680.
39. Mogami H, Tepikin AV, Petersen OH: **Termination of cytosolic Ca2+ signals: Ca2+ reuptake into intracellular stores is regulated by the free Ca2+ concentration in the store lumen.** *EMBO J* 1998, **17:**435-442.
40. Haugh JM, Codazzi F, Teruel M, Meyer T: **Spatial sensing in fibroblasts mediated by 3′ phosphoinositides.** *J Cell Biol* 2000, **151:**1269-1280.